Journal of King Saud University – Science (2017) **29**, 174–181

King Saud University
Journal of King Saud University – Science
www.ksu.edu.sa
www.sciencedirect.com

ORIGINAL ARTICLE

Radioactivity of ^{226}Ra, ^{232}Th, ^{40}K and ^{137}Cs in beach sand and sediment near to desalination plant in eastern Saudi Arabia: Assessment of radiological impacts

Fatimh Alshahri

Department of Physics, College of Science, University of Dammam, Dammam 1982-31441, Saudi Arabia

Received 26 February 2016; accepted 16 August 2016
Available online 21 August 2016

KEYWORDS

Natural radionuclides;
^{137}Cs;
Sand;
Sediment;
Desalination plant;
Saudi Arabia

Abstract Sand and sediment samples were collected from different locations along the beach near to desalination plant, which is one of the oldest and largest reverse osmosis desalination plants in Saudi Arabia, where the fluid waste is discharged. The activity concentrations of ^{226}Ra, ^{232}Th, ^{40}K and ^{137}Cs were measured using gamma-ray spectrometry. Radiation hazard indices were calculated to evaluate the radiological risk for the public and environment. This study is the first to evaluate the radiological impacts in the area under investigation. The mean values of radium equivalent activity (Ra_{eq}) were 74.1 Bq kg^{-1} for surface sand samples, 78.8 Bq kg^{-1} for subsurface sand samples and 78.1 Bq kg^{-1} for sediments. The mean values of gamma absorbed dose rate (D) in air and annual effective dose (E) for analyzed samples were lower than the acceptable values. The external radiation hazard indices were lower than unity for all samples.

1. Introduction

Desalination of sea or ocean water is a widespread technology used in many countries around the world. The desalination process is one of mankind's earliest designs to separate fresh water from a salt-water solution (Einav et al., 2002). Desalination involves several processes to remove the excess salt and other minerals from the water to obtain potable water for human usage.

Essentially, a desalination plant is a system to separate saline water into two streams: one with a low concentration of dissolved salts and inorganic materials and the other containing the remaining dissolved salts (brine). The amount of flow

Abbreviations: MDA, minimum detectable activity; UNSCEAR, United Nations Scientific Committee on the Effects of Atomic Radiation; WHO, World Health Organization.

E-mail address: faalshehri@uod.edu.sa

Peer review under responsibility of King Saud University.

ELSEVIER Production and hosting by Elsevier

http://dx.doi.org/10.1016/j.jksus.2016.08.005

discharged to waste as a brine discharge varies from 20 to 70 percent of the feed flow, depending on the technology used in the plant. Brine discharge is the fluid waste from a desalination plant, which contains a high percentage of salt and dissolved minerals (Mohamed et al., 2005). The brine returns to the sea and spreads according to different aspects (wind direction, wave height and tidal). Desalination plants could have several impacts on the surrounding environment. The major concern of these impacts near the outfall brine discharge due to its physical and chemical features (Younos, 2005; Abdul-Wahab, 2007; WHO, 2007).

Radiation and radioactivity in the environment have natural and man-made sources. Exposure to natural radiation represents the most significant part of the total exposure to radiation in the environment (Saleh, 2012; UNSCEAR, 2008). Only natural radionuclides with half-lives comparable with the age of the earth or their corresponding decay products existing in terrestrial material such as ^{232}Th, ^{238}U, ^{235}U, ^{226}Ra, ^{228}Ra and ^{40}K are of great interest. The levels of these radionuclides are relatively distributed in soil based on the nature of its geological formations (Al-Jundi et al., 2003; Orabi et al., 2006).

The Residual Saline Stream contains a range of contaminants, including naturally occurring radioactive materials (NORMs) that may increase the natural radioactivity levels along the shore line. Treatment processes such as dewatering, ion exchange, reverse osmosis, and other volume reduction may concentrate radionuclides to a level of concern (Hamidalddin, 2013). Long-lived radioactive elements such as uranium, thorium and potassium and any of their decay products, (e.g., radium and radon), are examples of NORM. These elements have always been present in the earth's crust and atmosphere. The ^{238}U series decay via a chain containing eight alpha decays and six beta decays to ^{206}Pb (Hamdy et al., 2007; Ahmed and El-Arabi, 2005; UNSCEAR, 1993, 2008).

The radiological impact from the natural radioactivity is due to radiation exposure of the body by gamma-rays and irradiation of lung tissues from the inhalation of radon and its progeny. From the natural risk point of view, it is necessary to know the dose limits of public exposure and to measure the natural environmental radiation level provided by ground, air, water, foods, building interiors, etc., to estimate human exposure to natural radiation sources (Akhtar and Tufail, 2011; El-Taher, 2010). Many studies have been conducted on the concentrations of natural radionuclides in the marine environment in different regions around the world (Price et al., 1998; Higgy, 1999; Sroor et al., 2001; Santawamaitre et al., 2011; Hamzah et al., 2011; Obhodas et al., 2012).

Saudi Arabia is the world's largest producer of desalinated seawater. The Saline Water Conversion Office (SWCO) constructed twenty-four desalination plants along the Saudi Arabian coasts, including the twelve major plants on the western coast on the Red Sea and another three on the eastern coast on the Arabian Gulf. The major three desalination plants in Saudi Arabia are Al-Jubail and Al-Khobar plants on the Arabian Gulf coast and Shoaiba plant on the Red Sea coast.

Al-Khobar desalination plant is located near an important beach, which is situated in the eastern region of Saudi Arabia. This beach is constantly frequented by the general population and many fishermen. In addition, a large number of palm trees spread along the beach. Therefore, this investigation aims to determine radionuclide levels along the beach near to desalination plant where the fluid waste is discharged and evaluate the radiation hazard indexes due to the radionuclides in the beach sand and sediment to identify the area that may be hazardous for public. In addition, these data will be useful for subsequent evaluations of possible future environmental contamination due to non-nuclear industries or any future activities.

2. Materials and methods

2.1. Samples collection and preparation

Thirty-six beach sand and sediments samples were collected from different locations along the beach near the desalination plant with a length interval of 6500 m (Fig. 1). Twenty-four sand samples were collected at 2 m from the shoreline. These samples were taken from surface and subsurface (10–30 cm). From the same locations, 12 sediment samples were collected from seawater at 2 m from the shoreline. Samples were bulked as a single sample and dried in an oven at 70 °C for 24 h. After that, samples were prepared for radiation counting by sieving through 2 mm mesh. Each sample was packed into 152 ml standard size beakers and tightly sealed and stored for 28 days to acquire secular equilibrium between ^{226}Ra and its progenies. Two reference materials were packed into the same standard size beakers for efficiency calibration.

2.2. Experimental setup

A hyper-pure Germanium detector (HPGe), coaxial type, p-type with relative efficiency of 20% was used. The detector is shielded with a low-level background lead shield. The HPGe was calibrated for efficiency using the reference material RGU-1 from IAEA. The certified activity of uranium is 400 ppm which is equivalent to 4960 Bq kg^{-1}. The energy transitions of the ^{226}Ra daughters (^{214}Pb and ^{214}Bi) were used to develop the efficiency calibration curve. A fourth degree polynomial fitting was performed to reach the best R^2 value ($\approx$0.976).

2.3. Gamma-spectrometric analysis

After subtracting the background, the radionuclides were measured at the gamma lines (Table 1). ^{226}Ra was measured using its progenies ^{214}Pb with energies 295.2 keV (19.3%) and 351.93 keV (37.6%), and ^{214}Bi with energies 609.31 keV (46.1%), 1120.29 keV (15.1%) and 1764.49 keV (15.4%). Radium was determined based on the above mentioned energy transitions after achieving secular equilibrium for 28 days after sample packing. For ^{232}Th, the specific activity concentration was determined using the gamma lines 338.40 keV (12.4%) and 911.07 keV (25.8%) for ^{228}Ac and 583.14 keV (33.1%) for ^{208}Tl. The average values were calculated. In the case of ^{40}K and ^{137}Cs, the specific activity concentrations were estimated directly by their gamma lines of 1460.75 keV (10.7%) and 661.7 keV (85.12%), respectively.

The software used for analysis and reduction of the gamma-ray spectra was Quantum Gold, Version 4.04.00.

The minimum detectable activity (MDA) for each isotope (^{226}Ra, ^{232}Th, ^{40}K and ^{137}Cs) in the background was calculated

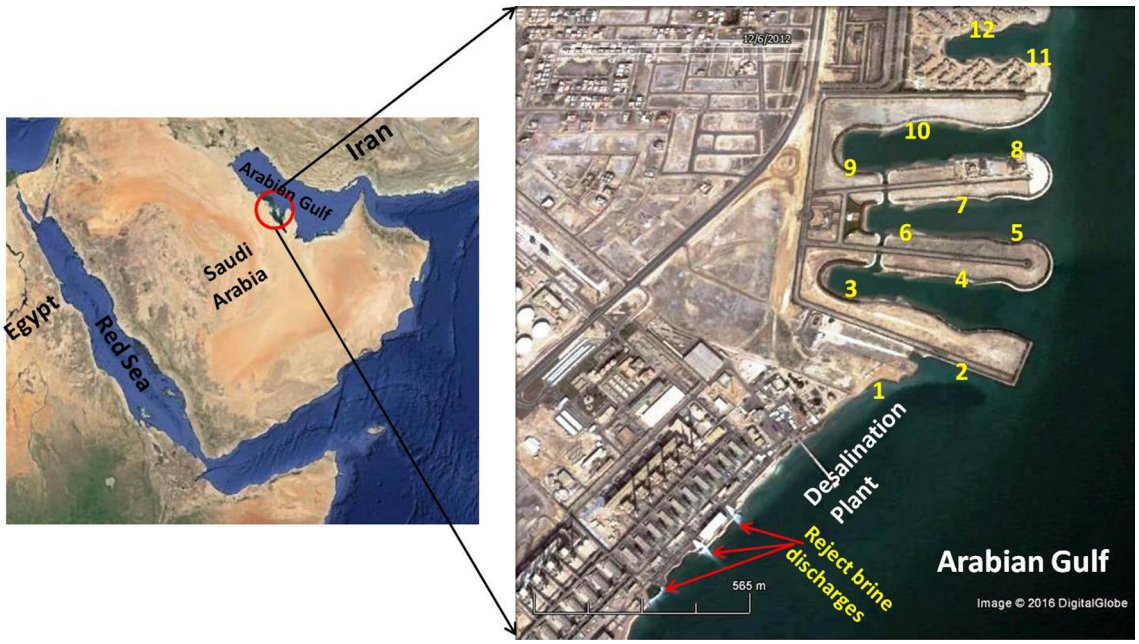

Figure 1 Location map of the collected samples along the beach near to desalination plant.

Table 1 Gamma rays and their related isotopes used to calculate the activity concentrations of the nuclides in the first column (Mansour et al., 2012; Saad and Al-Azmi, 2002).

Nuclide	Half-life (yr)	Gamma ray energy (keV)	Isotope	Intensity (%)
^{226}Ra	1650	295.2	^{214}Pb	19.3
		351.93	^{214}Pb	37.6
		609.31	^{214}Bi	46.1
		1120.29	^{214}Bi	15.1
		1764.49	^{214}Bi	15.4
^{232}Th	1.405×10^{10}	338.40	^{228}Ac	12.4
		583	^{208}Tl	33.1
		911.07	^{228}Ac	29.0
^{40}K	1.277×10^{9}	1460.83	^{40}Ar	10.7
^{137}Cs	30.17	661.66	^{137}Ba	85.2

separately based on the sample's weight (0.0332 kg) using the detection limit according to the formula (Currie, 1989):

$$\mathrm{MDA(Bq)} = \frac{2.7 + 4.65\sqrt{\mathrm{BG}}}{\varepsilon I_\gamma t} \quad (1)$$

where BG is the background count below the peak of interest, ε is the absolute efficiency, I_γ is the gamma line intensity and t is the counting time in second. The MDAs for ^{226}Ra, ^{232}Th, ^{40}K and ^{137}Cs were 0.05, 0.03, 0.16 and 0.09 Bq kg^{-1}, respectively.

To assess the radiological hazard associated with sand samples and sediments of the studied area, it is useful to calculate an index called the radium equivalent activity, $\mathrm{Ra_{eq}}$. It can be calculated from the following relation (Boukhenfouf and Boucenna, 2011; Alshahri and Alqahtani, 2015):

$$\mathrm{Ra_{eq}\ (Bq\ kg^{-1})} = \mathrm{A_{Ra}} + 1.43\mathrm{A_{Th}} + 0.077\mathrm{A_K} \quad (2)$$

where $\mathrm{A_{Ra}}$, $\mathrm{A_{Th}}$ and $\mathrm{A_K}$ are the specific activities of ^{226}Ra, ^{232}Th and ^{40}K, respectively, expressed in Bq kg^{-1}.

The absorbed dose rate in air 1 m above the ground surface for the radionuclides (^{232}Th, ^{226}Ra, and ^{40}K) was computed on the basis of guidelines provided by Ahmed and El-Arabi (2005). The conversion factors used to compute the absorbed dose rates (D) in air per unit activity concentration in 1 Bq kg^{-1} sand correspond to 0.666 nGy h^{-1} for ^{232}Th, 0.429 nGy h^{-1} for ^{226}Ra, and 0.0417 nGy h^{-1} for ^{40}K. Therefore, D could be obtained from the following relation:

$$\mathrm{D\ (nGy\ h^{-1})} = 0.429\ \mathrm{A_{Ra}} + 0.666\mathrm{A_{Th}} + 0.0417\mathrm{A_K} \quad (3)$$

where $\mathrm{A_{Ra}}$, $\mathrm{A_{Th}}$ and $\mathrm{A_K}$ are the activity concentrations of ^{226}Ra, ^{232}Th and ^{40}K (Bq kg^{-1}), respectively.

The annual effective dose rate E (mSv y^{-1}) received by the population is calculated using the following equation (UNSCEAR, 2000):

$$\mathrm{E(mSv\ y^{-1})} = \mathrm{D(nGy\ h^{-1})} \times 8760\mathrm{(h\ y^{-1})} \times 0.2 \times 0.7\mathrm{(Sv\ Gy^{-1})} \times 10^{-6} \quad (4)$$

where D (nGy h^{-1}) is the absorbed dose rate in air, 8760 h is the time for one year, 0.7 (Sv Gy^{-1}) is the conversion factor, which converts the absorbed dose rate in air to human effective dose and 0.2 is the outdoor occupancy factor (UNSCEAR, 2000).

Another radiation hazard index is called the external hazard index (H_{ex}). This index due to external exposure to gamma rays from the studied sand and sediment samples, which must be less than unity. H_{ex} is defined as the following (AlZahrani et al., 2011):

$$H_{ex} = \frac{\mathrm{A_{Ra}}}{370} + \frac{\mathrm{A_{Th}}}{259} + \frac{\mathrm{A_K}}{4810} \leqslant 1 \quad (5)$$

where $\mathrm{A_{Ra}}$, $\mathrm{A_{Th}}$ and $\mathrm{A_K}$ are the activity concentrations of ^{226}Ra, ^{232}Th and ^{40}K (Bq kg^{-1}), respectively.

3. Results and discussion

3.1. Activity concentrations of ^{226}Ra, ^{232}Th, ^{40}K and ^{137}Cs in sand samples and sediment

The activity concentrations of ^{226}Ra, ^{232}Th, ^{40}K and ^{137}Cs were determined for sand samples and sediment (Tables 2–4). The activity concentrations of ^{226}Ra ranged from 12.1 ± 1.3 to 36.3 ± 3.3 Bq kg^{-1} with a mean value of 22.7 ± 2.8 Bq kg^{-1} for sand samples collected from surface and from 19.3 ± 2.5 to 31.4 ± 3.4 Bq kg^{-1} with a mean value of 23.9 ± 2.9 Bq kg^{-1} for subsurface samples. The highest activity concentration of Radium was found to be 36.3 ± 3.3 Bq kg^{-1} for the sample S3 which was collected from the surface at site 3. The activity concentrations of ^{232}Th ranged from 9.30 ± 0.9 to 26.9 ± 5.6 Bq kg^{-1} with a mean value of 14.8 ± 2.3 Bq kg^{-1} for sand samples from surface and from 8.7 ± 1.0 to 17.3 ± 2.1 Bq kg^{-1} with a mean value of 12.8 ± 1.8 Bq kg^{-1} for subsurface samples. The concentrations of ^{40}K and ^{137}Cs for surface samples ranged from 261 ± 10 to 454 ± 17 Bq kg^{-1} and from below the MDA to 1.38 ± 0.15 Bq kg^{-1}, respectively. Similarly, the concentrations of ^{40}K and ^{137}Cs for subsurface sand samples ranged from 358 ± 14 to 686 ± 21 Bq kg^{-1} and from below the MDA to 0.97 ± 0.12 Bq kg^{-1}, respectively.

For sediment samples, the activity concentrations ranged from 18.3 ± 1.6 to 37.6 ± 4.5 Bq kg^{-1} with a mean value of 26.4 ± 2.8 Bq kg^{-1} for ^{226}Ra, from 7.8 ± 1.3 to 25.5 ± 3.7 Bq kg^{-1} with a mean value of 16.3 ± 2.2 Bq kg^{-1} for ^{232}Th, from 202 ± 11 to 432 ± 15 Bq kg^{-1} with a mean value of 351 ± 15 Bq kg^{-1} for ^{40}K and from below the MDA to 2.16 ± 0.25 Bq kg^{-1} for ^{137}Cs.

The obtained results show that the mean values of ^{40}K concentrations in sand samples were higher than the range of the world average 370 Bq kg^{-1}. The activity levels of ^{137}Cs were found to be lower than the minimum detection limit in most of sand and sediment samples. The slight appearance of ^{137}Cs was observed in the measured samples which may be due to the fertilized soil in the investigated area (Boukhenfouf and Boucenna, 2011). The variations in activity concentrations of ^{226}Ra, ^{232}Th and ^{40}K in sand samples based on the nature of its geological formations and may be due to the result of the depositional processes of radionuclides and heavy minerals along the shoreline during the high tide.

Table 2 Activity concentration in Bq kg^{-1} of ^{226}Ra, ^{232}Th, ^{40}K and ^{137}Cs for sand samples collected from surface along the beach near to desalination plant.

Sample code	Lat.	Long.	^{226}Ra	^{232}Th	^{40}K	^{137}Cs
S1	N: 26°10′54.03″	E: 50°13′01.03″	12.1 ± 1.3	10.1 ± 1.3	261 ± 10	< MDA
S2	N: 26°10′57.29″	E: 50°13′05.83″	21.3 ± 2.3	9.73 ± 0.9	454 ± 17	1.38 ± 0.15
S3	N: 26°10′00.88″	E: 50°13′52.72″	36.3 ± 3.3	26.9 ± 5.6	416 ± 13	0.54 ± 0.06
S4	N: 26°11′01.92″	E: 50°13′08.44″	21.5 ± 1.3	9.80 ± 0.9	454 ± 17	< MDA
S5	N: 26°11′07.15″	E: 50°13′07.74″	29.3 ± 3.2	12.1 ± 1.3	377 ± 15	0.64 ± 0.08
S6	N: 26°11′11.05″	E: 50°12′54.19″	15.0 ± 2.3	9.30 ± 1.0	408 ± 12	< MDA
S7	N: 26°°11′12.07″	E: 50°13′03.56″	18.1 ± 2.2	11.1 ± 1.7	369 ± 11	< MDA
S8	N: 26°11′17.35″	E: 50°13′10.21″	21.6 ± 3.0	16.5 ± 3.1	335 ± 12	< MDA
S9	N: 26°11′19.12″	E: 50°12′49.47″	27.9 ± 5.8	16.7 ± 2.8	416 ± 12	< MDA
S10	N: 26°11′22.07″	E: 50°13′00.48″	30.6 ± 3.4	22.7 ± 3.6	435 ± 13	< MDA
S11	N: 26°11′30.07″	E: 50°13′11.24″	22.5 ± 2.4	20.7 ± 3.1	352 ± 12	< MDA
S12	N: 26°11′33.87″	E: 50°13′05.14″	16.1 ± 1.8	12.1 ± 1.9	426 ± 13	< MDA
Min			12.1 ± 1.3	9.30 ± 0.9	261 ± 10	< MDA
Max			36.3 ± 3.3	26.9 ± 5.6	454 ± 17	1.38 ± 0.15
Mean			22.7 ± 2.8	14.8 ± 2.3	392 ± 13	–

Table 3 Activity concentration in Bq kg^{-1} of ^{226}Ra, ^{232}Th, ^{40}K and ^{137}Cs for sand samples collected from subsurface along the beach near to desalination plant.

Sample code	Lat.	Long.	^{226}Ra	^{232}Th	^{40}K	^{137}Cs
SB1	N: 26°10′54.03″	E: 50°13′01.03″	19.5 ± 2.9	15.5 ± 2.3	416 ± 17	< MDA
SB2	N: 26°10′57.29″	E: 50°13′05.83″	20.7 ± 2.7	12.9 ± 2.1	377 ± 15	< MDA
SB3	N: 26°10′00.88″	E: 50°13′52.72″	20.6 ± 2.7	10.3 ± 1.3	686 ± 21	< MDA
SB4	N: 26°11′01.92″	E: 50°13′08.44″	19.3 ± 2.5	12.3 ± 1.5	504 ± 15	< MDA
SB5	N: 26°11′07.15″	E: 50°13′07.74″	23.9 ± 2.8	9.80 ± 1.1	416 ± 13	< MDA
SB6	N: 26°11′11.05″	E: 50°12′54.19″	22.2 ± 2.4	10.1 ± 1.1	358 ± 14	< MDA
SB7	N: 26°11′12.07″	E: 50°13′03.56″	24.5 ± 2.9	14.9 ± 2.3	506 ± 15	< MDA
SB8	N: 26°11′17.35″	E: 50°13′10.21″	31.4 ± 3.4	16.6 ± 3.0	437 ± 16	< MDA
SB9	N: 26°11′19.12″	E: 50°12′49.47″	27.3 ± 3.1	8.70 ± 1.0	421 ± 13	< MDA
SB10	N: 26°11′22.07″	E: 50°13′00.48″	29.1 ± 3.2	17.3 ± 2.1	387 ± 12	0.97 ± 0.12
SB11	N: 26°11′30.07″	E: 50°13′11.24″	30.1 ± 3.9	16.2 ± 2.2	472 ± 16	< MDA
SB12	N: 26°11′33.87″	E: 50°13′05.14″	24.5 ± 3.1	17.3 ± 2.4	404 ± 12	0.85 ± 0.09
Min			19.3 ± 2.5	8.70 ± 1.0	358 ± 14	< MDA
Max			31.4 ± 3.4	17.3 ± 2.1	686 ± 21	0.97 ± 0.12
Mean			23.9 ± 2.9	12.8 ± 1.8	451 ± 15	–

Table 4 Activity concentration in Bq kg^{-1} of ^{226}Ra, ^{232}Th, ^{40}K and ^{137}Cs for sediment samples.

Sample code	Lat.	Long.	^{226}Ra	^{232}Th	^{40}K	^{137}Cs
SD1	N: 26°10′54.03″	E: 50°13′01.03″	23.5 ± 2.8	16.0 ± 2.2	275 ± 11	< MDA
SD2	N: 26°10′57.29″	E: 50°13′05.83″	22.9 ± 2.7	15.9 ± 1.5	280 ± 11	< MDA
SD3	N: 26°10′00.88″	E: 50°13′52.72″	25.6 ± 3.1	15.4 ± 3.1	420 ± 17	2.16 ± 0.25
SD4	N: 26°11′01.92″	E: 50°13′08.44″	18.3 ± 1.6	9.50 ± 1.0	432 ± 15	1.27 ± 0.15
SD5	N: 26°11′07.15″	E: 50°13′07.74″	24.1 ± 2.8	14.9 ± 1.9	355 ± 18	1.04 ± 0.12
SD6	N: 26°11′11.05″	E: 50°12′54.19″	26.3 ± 3.2	14.1 ± 1.8	417 ± 21	< MDA
SD7	N: 26°11′12.07″	E: 50°13′03.56″	31.9 ± 2.9	20.1 ± 1.9	383 ± 19	1.20 ± 0.14
SD8	N: 26°11′17.35″	E: 50°13′10.21″	24.0 ± 3.1	7.80 ± 1.3	386 ± 15	< MDA
SD9	N: 26°11′19.12″	E: 50°12′49.47″	37.6 ± 4.5	25.5 ± 3.7	386 ± 16	< MDA
SD10	N: 26°11′22.07″	E: 50°13′00.48″	22.9 ± 2.1	16.3 ± 2.1	202 ± 11	< MDA
SD11	N: 26°11′30.07″	E: 50°13′11.24″	23.7 ± 2.6	15.3 ± 3.3	385 ± 17	< MDA
SD12	N: 26°11′33.87″	E: 50°13′05.14″	35.4 ± 3.1	25.1 ± 2.6	294 ± 13	< MDA
Min			18.3 ± 1.6	7.80 ± 1.3	202 ± 11	< MDA
Max			37.6 ± 4.5	25.5 ± 3.7	432 ± 15	2.16 ± 0.25
Mean			26.4 ± 2.8	16.3 ± 2.2	351 ± 15	–

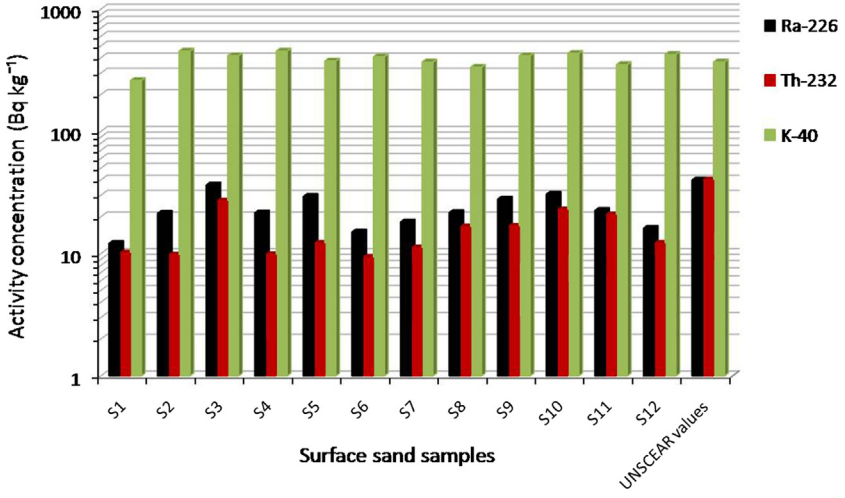

Figure 2 Distribution of ^{226}Ra, ^{232}Th and ^{40}K in surface sand samples along the beach and the allowed values by UNSCEAR (2000).

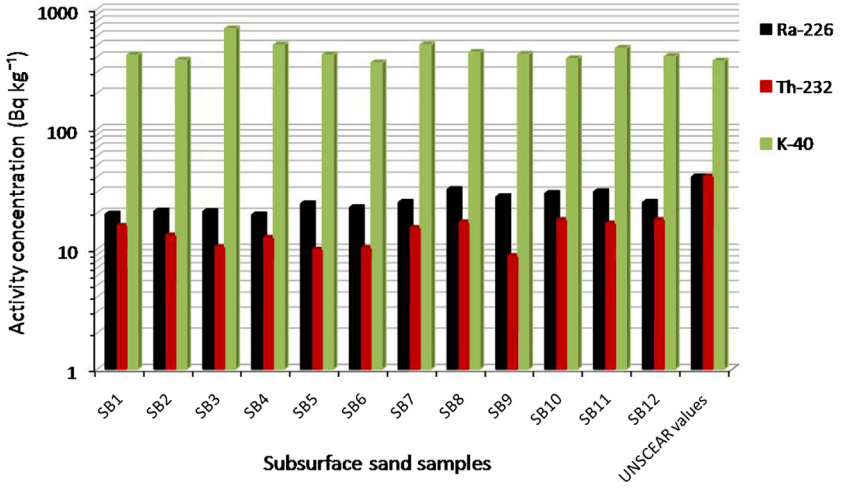

Figure 3 Distribution of ^{226}Ra, ^{232}Th and ^{40}K in subsurface sand samples along the beach and the allowed values by UNSCEAR (2000).

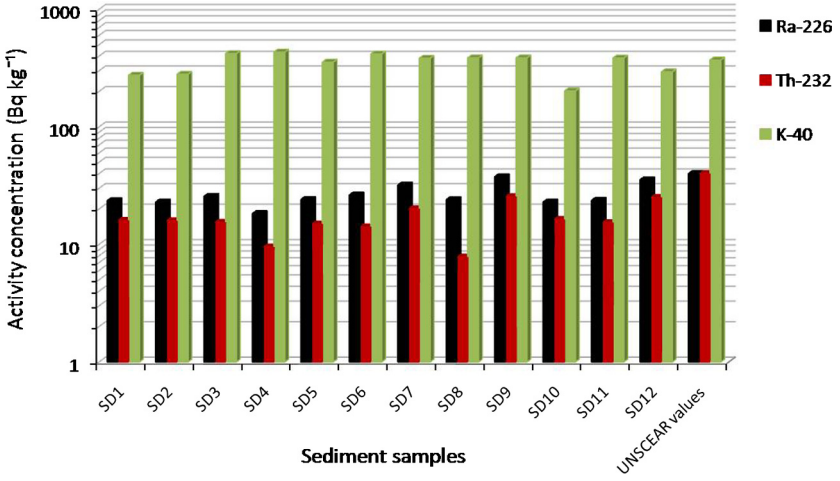

Figure 4 Distribution of ^{226}Ra, ^{232}Th and ^{40}K in sediment samples along the beach and the allowed values by UNSCEAR (2000).

Table 5 Mean values of radium equivalent activity (Bq kg^{-1}), absorbed gamma radiation dose rate in air (nGy h^{-1}), annual effective dose (mSv y^{-1}), and external radiation hazard index (H_{ex}) for sand samples and sediment.

Type of sample	Ra_{eq} (Bq kg^{-1})	D (nGy h^{-1})	E (mSv y^{-1})	H_{ex}
Sand from surface	74.1	37.2	0.04	0.02
Subsurface sand	78.8	38.3	0.05	0.21
Sediment	78.1	36.7	0.05	0.21
World's average (UNSCEAR, 1993, 2000)	370	55	1	$\leqslant$1

Table 6 Comparison of mean and range activity concentration (Bq kg^{-1}) in sand samples and sediment with those in other studies.

Region (Ref.)	Depth	^{226}Ra	^{232}Th	^{40}K
Red sea, Saudi Arabia (Hamidalddin, 2013)	Surface	14.22 ± 0.65	14.00 ± 0.45	968.19 ± 0.14
	50 cm	24.34 ± 0.12	17.3 ± 0.15	934.45 ± 0.61
Farasan Island coast, Saudi Arabia (Al-Zahrany et al., 2012)	Sediment	3.31	1.84	34.34
Coast of Kuwait (Saad and Al-Azmi, 2002)	Surface	36 (8–72)	6 (2–17)	227 (41–492)
Libya beach (El-Kameesy et al., 2008)	5–10	7.5 ± 2.5	4.5 ± 1.3	28.5 ± 6.7
	50–70	6.7 ± 1.9	4.2 ± 1.1	26.6 ± 5.9
Al-Khafji and Mneefa coast, Saudi Arabia (Al-Kheliewi et al., 2002)	0–10 cm	2.61–7.53	0.19 ± 0.05–0.82 ± 0.08	27.04 ± 1.73–204.2 ± 4.4
	12–25 cm	1.99–9.46	0.15–0.95	23.69–253.3
Red sea, Egypt (Harb, 2008)	0–30 cm	22.7	12.4	930
Mediterranean Coast, Turkey (Ozmen et al., 2014)	Surface	4.0 ± 0.5–21.5 ± 1.8	1.8 ± 0.4–27.9 ± 2.4	19.0 ± 2.2–590.3 ± 28.6
Inani Beach, Bangladesh (Ahmed et al., 2014)	10–15 cm	15.14 ± 2.62–28.67 ± 3.09	24.39 ± 2.50–49.46 ± 3.58	362.00 ± 79.61–560.87 ± 81.40
Coast of Xiamen Island, China (Huang et al., 2015)	Surface	–	6.5–41.4	197.4–487.6
World's average (UNSCEAR, 2000)	–	40	40	370
Present work (sand samples collected at 2 m from the shoreline)	Surface	22.7 ± 2.8	14.8 ± 2.3	392 ± 13
	Subsurface	23.9 ± 2.9	12.8 ± 1.8	451 ± 15
Present work (sediment)	–	26.4 ± 2.8	16.3 ± 2.2	351 ± 15

The distributions of radium, thorium and potassium activities in all sand and sediment samples are given in Figs. 2–4. These figures compare between the values of this study and the allowed values in soil as considered by UNSCEAR (2000). The result showed that the highest values of potassium were found in subsurface samples.

3.2. Radiation hazard indexes

The radium equivalent activity (Ra_{eq}), total absorbed dose rate in air 1 m above the ground (D), annual effective dose (E) and external hazard index (H_{ex}) were calculated for all sand and sediment samples, the mean values of the above radiation

hazard indexes are shown in Table 5. The mean values of radium equivalent activity, Ra_{eq}, were 74.1, 78.8 and 78.1 Bq kg^{-1} for surface sand, subsurface sand and sediment which were lower than the acceptable value of 370 Bq kg^{-1} (UNSCEAR, 1993). The mean values of gamma adsorbed dose rate (D) in air and annual effective dose (E) for sand samples from surface were 37.2 nGy h^{-1} and 0.04 mSv y^{-1}, respectively, and for sand samples from subsurface were 38.3 nGy h^{-1} and 0.05 mSv y^{-1}, respectively. The mean values of gamma adsorbed dose rate D in air and annual effective dose (E) for sediment samples were 36.7 nGy h^{-1} and 0.05 mSv y^{-1}, respectively. These results were within the estimated average global terrestrial radiation of 55 nGy h^{-1} and the acceptable value of annual effective dose (1 mSv y^{-1}) for the public (UNSCEAR, 1993, 2000). The mean values of the external radiation hazard index (H_{ex}) for all samples were lower than unity. From these results, the radiological risk is insignificant due to the low values of gamma dose rates in all samples under investigation.

3.3. Comparison of activity concentrations with other studies

The mean values of the radioactivity levels were compared with the world average which are 40, 40 and 370 Bq kg^{-1} for ^{226}Ra, ^{232}Th and ^{40}K, respectively, (UNSCEAR, 2000). The measurements of all sand and sediment samples under investigation showed that the mean values of radioactivity levels were lower than the world average, expect the mean values of potassium in sand samples. In addition, the specific activities of ^{226}Ra, ^{232}Th and ^{40}K for the analyzed samples were compared with the similar investigations in other countries (Table 6). It can be seen that, the natural radioactivity levels fall within the range of published data from other countries.

4. Conclusions

In this study, the specific activities for ^{226}Ra, ^{232}Th, ^{40}K and ^{137}Cs were measured in 36 sand and sediment samples at different distances from a desalination plant along the beach, eastern Saudi Arabia, using gamma-ray spectrometry. The measurements of all samples under investigation showed that the mean values of radioactivity levels were lower than the world average for ^{226}Ra, ^{232}Th, ^{40}K and ^{137}Cs, except the mean values of ^{40}K concentration in sand samples. However, the mean values of radium equivalent activity (Ra_{eq}), total absorbed dose rate in air 1 m above the ground (D), annual effective dose (E) and external hazard index H_{ex} were found to be within the allowed limits (UNSCEAR, 1993, 2008). In view of the current study, the radiological impacts of radionuclides in the beach near to desalination plant are negligible compared to the acceptable values (UNSCEAR, 1993, 2008). Thus, sand and sediments in the area near to disposal site of the fluid waste from desalination plant would not pose any significant source of radiation hazard to the population.

Acknowledgements

The author greatly appreciates the work performed by Ameena Alahmari from the radiation laboratory, University of Dammam. I am also grateful to Dr. Hanadi Baghdadi, director of the Research units, University of Dammam, for her support and help during this study.

Appendix A. Supplementary data

Supplementary data associated with this article can be found, in the online version, at http://dx.doi.org/10.1016/j.jksus.2016.08.005.

References

Abdul-Wahab, S.A., 2007. Characterization of water discharges from two thermal power/desalination plants in Oman. Eng. Sci. 24, 321–337.

Ahmed, N.K., El-Arabi, A.G.M., 2005. Natural radioactivity in farm soil and phosphate fertilizer and its environmental implications in Qena governorate, Upper Egypt. J. Environ. Radioact. 84, 51–64.

Ahmed, M.M., Das, S.K., Haydar, M.A., Bhuiyan, M.M.H., Ali, M. I., Paul, D., 2014. Study of natural radioactivity and radiological hazard of sand, sediment, and soil samples from Inani beach, Cox's Bazar, Bangladesh. J. Nucl. Part. Phys. 4 (2), 69–78.

Akhtar, N., Tufail, M., 2011. Cancer risk in Pakistan due to natural environmental pollutants. Int. J. Environ. Res. 5 (1), 159–166.

Al-Jundi, J., Al-Bataina, B.A., Abu-Rukah, Y., Shehadeh, H.M., 2003. Natural radioactivity concentrations in soil samples along the Amman Aqaba Highway, Jordan. Radiat. Measur. 36, 555–560.

Al-Kheliewi, A.S., Farouk, M.A., Al-Zahrany, A.A., Shabana, S.I., 2002. Levels at the Al-Khafji and Mneefa coastal areas in Saudi Arabia. In: The 6th Saudi Engineering Conference. KFUPM, Dhahran.

Alshahri, F., Alqahtani, M., 2015. Chemical fertilizers as a source of ^{238}U, ^{40}K, ^{226}Ra, ^{222}Rn and trace metal pollutant of the environment in Saudi Arabia. Environ. Sci. Pollut. Res. 22, 8339–8348.

AlZahrani, J.H., Alharbi, W.R., Abbady, A.G.E., 2011. Radiological impacts of natural radioactivity and heat generation by radioactive decay of phosphorite deposits from northwestern Saudi Arabia. Aust. J. Basic Appl. Sci. 5 (6), 683–690.

Al-Zahrany, A.A., Farouk, M.A., Al-Yousef, A.A., 2012. Distribution of naturally occurring radioactivity and ^{137}Cs in the marine sediment of farasan island, southern Red Sea, Saudi Arabia. Radiat. Prot. Dosimetry 152 (1–5), 135–139.

Boukhenfouf, W., Boucenna, A., 2011. The radioactivity measurements in soils and fertilizers using gamma spectrometry technique. J. Environ. Radioact. 102, 336–339.

Currie, L.A., 1989. Limits for qualitative detection and quantitative determination application to radiochemistry. Anal. Chem. 40, 586–593.

Einav, R., Harussi, K., Perry, D., 2002. The footprint of the desalination processes on the environment. Desalination 152, 141–154.

El-Kameesy, S.U., Abd El-Ghany, S., El-Minyawi, S.M., Miligy, Z., El-Mabrouk, E.M., 2008. Natural radioactivity of beach sand samples in the Tripoli region, Northwest Libya, Turkish. J. Eng. Environ. Sci. 32, 245–251.

El-Taher, A., 2010. Gamma spectroscopic analysis and associated radiation hazards of building materials used in Egypt. Radiat. Prot. Dosimetry 138 (2), 158–165.

Hamdy, A., Diab, H.M., El-Fiki, S.A., Nouh, S.A., 2007. Natural Radioactivity in the Cultivated Land Around the Fertilizer Factory. The Second All African IRPA Regional Radiation Protection Congress, Ismailia, Egypt.

Hamidalddin, S.H.Q., 2013. Measurements of the natural radioactivity along Red Sea coast (South beach of Jeddah Saudi Arabia). Life Sci. J. 10 (1), 121–128.

Hamzah, Z., Abdul Rahman, S.A., Saat, A., 2011. Measurement of ^{226}Ra, ^{228}Ra and ^{40}K in soil in district of Kuala Krai, using gamma spectrometry, Malaysian. J. Anal. Sci. 15 (2), 159–166.

Harb, S., 2008. Natural radioactivity and external gamma radiation exposure at the coastal Red Sea in Egypt. Radiat. Prot. Dosimetry 130 (3), 376–384.

Higgy, R.H., 1999. Natural radionuclides in soil and shore sediments on Alexandria Mediterranean Sea coast of Egypt. In: 16th National Radio Science Conference. NRsC'99 Ain Shams University, Cairo, Egypt.

Huang, Y., Lu, X., Ding, X., Feng, T., 2015. Natural radioactivity level in beach sand along the Coast of Xiamen Island, China. Mar. Pollut. Bull. 91 (1), 357–361.

Mansour, N.A., Ahmed, T.S., Fayez-Hassan Nabil, M., Hassan, M., Gom, M.A., Ali, A., 2012. Measurements of radiation level around the location of norm in solid wastes at petroleum companies in Egypt. J. Am. Sci. 8 (6), 252–261.

Mohamed, A.M.O., Maraqa, M., Al Handhaly, J., 2005. Impact of land disposal of reject brine from desalination plants on soil and groundwater. Desalination 182, 411–433.

Obhodas, J., Valkovic, V., Matjacic, L., Nad, K., Sudac, D., 2012. Evaluation of elemental composition of sediments from the Adriatic Sea by using EDXRF technique. Appl. Radiat. Isot. 70 (7), 1392–1395.

Orabi, H., Al-Shareaif, A., El Galefi, M., 2006. Gamma-ray measurements of naturally occurring radioactive sample from Alkharje city. J. Radioanal. Nucl. Chem. 269, 99–102.

Ozmen, S.F., Cesur, A., Boztosun, C.I., Yavuz, C.M., 2014. Distribution of natural and anthropogenic radionuclides in beach sand samples from mediterranean coast of Turkey. Radiat. Phys. Chem. 103, 37–44.

Price, A.R.G., Jobbins, G., Dawson Shepherd, A., Ormond, R.F.G., 1998. An integrated environmental assessment of the Red Sea coast of Saudi Arabia. Environ. Concerv. 25 (1), 65–76.

Saad, H.R., Al-Azmi, D., 2002. Radioactivity concentrations in sediments and their correlation to the coastal structure in Kuwait. Appl. Radiat. Isot. 56, 991–997.

Saleh, I.H., 2012. Radioactivity of ^{238}U, ^{232}Th, ^{40}K, and ^{137}Cs and assessment of depleted uranium in soil of the Musandam Peninsula, Sultanate of Oman. Turkish J. Eng. Environ. Sci. 36, 236–248.

Santawamaitre, T., Malain, D., Al-Sulaiti, H.A., Matthews, M., Bradley, D.A., Regan, P.H., 2011. Study of natural radioactivity in riverbank soils along the Chao Phraya river basin in Thailand. Nucl. Instrum. Meth. Phys. Res. A652, 920–924.

Sroor, A., El-Bahi, S.M., Ahmed, F., Abdel-Haleem, A.S., 2001. Natural radioactivity and radon exhalation rate of soil in southern Egypt. Appl. Radiat. Isot. 55, 873–879.

UNSCEAR, 1993. Sources and effects of ionizing radiation. United Nations Scientific Committee on the effects of Atomic Radiation. Report to the general Assembly, United Nations, New York. Annex A, 18–33.

UNSCEAR, 2000. United Nations Scientific Committee on the Effects of Atomic Radiation. Sources and Effects of Ionizing Radiation. Report to the General Assembly, Annex A & B, vol. I, 20–141.

UNSCEAR, 2008. United Nations Scientific Committee on the Effects of Atomic Radiation. Report to the General Assembly United Nations, New York. Annex B, vol. I, 223–439.

WHO, 2007. Desalination for Safe Water Supply, Guidance for the Health and Environmental Aspects Applicable to Desalination. World Health Organization, Geneva. <http://www.who.int/water_sanitation_health/en>.

Younos, T., 2005. Environmental issues of desalination. J. Contemporary Water Res. Educ., 11–18, Universities Council on Water Resources UCOWR132